

High-dimensional Sparse Precision Matrix Estimation via Sparse Column Inverse Operator*

Weidong Liu and Xi Luo

Shanghai Jiao Tong University and Brown University

October 24, 2018

Abstract

This paper proposes a new method for estimating sparse precision matrices in the high dimensional setting. This procedure applies a novel Sparse Column-wise Inverse Operator (SCIO) to modified sample covariance matrices. We establish the convergence rates of this procedure under various matrix norms. Under the Frobenius norm loss, we prove theoretical guarantees on using cross validation to pick data-driven tuning parameters. Another important advantage of this estimator is its efficient computation for large-scale problems, using a path-following coordinate descent algorithm we provide. Numerical merits of our estimator are also illustrated using simulated and real datasets. In particular, this method is found to perform favorably on analyzing an HIV brain tissue dataset and an ADHD resting fMRI dataset.

Keywords: covariance matrix, precision matrix, cross validation, Frobenius norm, Gaussian graphical model, rate of convergence, spectral norm, lasso, HIV-1 associated neurocognitive disorders, ADHD resting fMRI.

*Weidong Liu is Professor, Department of Mathematics and Institute of Natural Sciences, Shanghai Jiao Tong University, Shanghai, CHINA. Xi Luo is Assistant Professor, Department of Biostatistics and Center for Statistical Sciences, Brown University, Providence, RI 02912, USA. WL's research was supported by the Program for Professor of Special Appointment (Eastern Scholar) at Shanghai Institutions of Higher Learning, the Foundation for the Author of National Excellent Doctoral Dissertation of PR China and the startup fund from SJTU. XL's research was supported by the startup fund from Brown University.

To whom correspondence should be addressed. Email: xluo@stat.brown.edu.

1 Introduction

Estimating covariance matrix and its inverse is fundamental in multivariate analysis. Among many interesting examples are principal component analysis, linear/quadratic discriminant analysis, and graphical models. In particular, the inverse covariance matrix (precision matrix) plays important roles in the latter two examples, and we will focus on estimating the precision matrix in this paper. Driven by recent advances on data collecting technologies, one often need to draw statistical inference on datasets with very large number of variables, much larger than the sample size. Under this setting, also known as high dimensional setting, it is no longer viable to invert the sample covariance to estimate the precision matrix. Computationally, even if such operation could be carried out, inverting a very large matrix is expensive in memory and time costs. To address these challenges in computation and estimation, we propose a new column-wise procedure that enjoys efficient computation while maintaining desirable convergence rates.

Let $\mathbf{X} = (X_1, \dots, X_p)$ be a p -variate random vector with a covariance matrix $\mathbf{\Sigma}$ and its corresponding precision matrix $\mathbf{\Omega} := \mathbf{\Sigma}^{-1}$. Suppose we observe an independent and identically distributed random sample $\{\mathbf{X}_1, \dots, \mathbf{X}_n\}$ from the distribution of \mathbf{X} . Various regularizations on the likelihood criterion have been proposed to stabilize the estimate for $\mathbf{\Omega}$. In particular, the ℓ_1 penalized normal likelihood estimator and its variants, which shall be called ℓ_1 -MLE estimators, were considered in several papers; see, for example, Yuan and Lin (2007), Friedman et al. (2008), Banerjee et al. (2008), and Rothman et al. (2008). Friedman et al. (2008) developed an efficient R package, *Glasso*, to compute the ℓ_1 -MLE. The convergence rate under the Frobenius norm loss was given in Rothman et al. (2008). Under the mutual incoherence or irrepresentable conditions, Ravikumar et al. (2011) obtained the rates of convergence in the elementwise ℓ_∞ norm and spectral norm. Nonconvex penalties, usually computationally more demanding, have also been considered under the same normal likelihood model. For example, Lam and Fan (2009) and Fan et al. (2009) considered penalizing the normal likelihood with the nonconvex SCAD penalty (Fan and Li, 2001). The main goal is to ameliorate the bias problem due to ℓ_1 penalization. One bottle neck in computing these estimators is its complex likelihood function.

Recently, column-wise or neighborhood based procedures has caught much attention because of the advantages in both computation and convergence rates. In an important paper, Meinshausen and Bühlmann (2006) demonstrated convincingly a neighborhood selection approach to recover the support of $\mathbf{\Omega}$ in a row by row fashion. For each row, the computation is reduced to run a ℓ_1 penalized least squares, aka LASSO (Tibshirani, 1996). This then can be solved efficiently via path-following coordinate descent (Friedman et al,

2008b). Yuan (2009) replaced the lasso selection by a Dantzig type modification, where first the ratios between the off-diagonal elements ω_{ij} and the corresponding diagonal element ω_{ii} were estimated for each row i and then the diagonal entries ω_{ii} were obtained given the estimated ratios. Convergence rates under the matrix ℓ_1 norm and spectral norm losses were established. This procedure can be solved via standard packages on linear programming. Cai, Liu and Luo (2011) proposed a procedure, CLIME, which seeks the sparsest precision matrix (measured by the ℓ_1 norm) within a modified feasible set of the ℓ_1 -MLE estimator. Their procedure is casted as a column-wise procedure, and each column is estimated via linear programming. They established the convergence rates of various norms without imposing the mutual incoherence conditions (Ravikumar et al. 2011), and proved improved convergence rates upon the ℓ_1 -MLE estimator when \mathbf{X} follows polynomial tail distributions. Even though Yuan (2009) and CLIME can be casted as linear programming, these problems are still computational expensive for really large p .

All these penalization methods require choosing some appropriate tuning parameters, also known as penalization parameters. Despite that these procedures are justified using asymptotic and finite-sample theories before, understanding of these procedures in practice is rather limited, as the theories are usually built on some theoretical choices of tuning parameters that cannot be implemented in practice. On the other hand, cross validation is probably the most widely employed data-driven scheme for choosing such parameters, however, the corresponding theory is sparse. Bickel and Levina (2008) analyzed the performance of thresholding covariance matrices, where the threshold is chosen using partial samples. A different approach using large sample theory was employed by Cai and Liu (2011), and they provided adaptive thresholding for covariance matrix estimation using the whole samples. Unfortunately, these results cannot be simply extended to the inverse covariance setting, due to the problem complexity. Exploiting the simplification brought by our column-wise procedures, this paper is among the first to demonstrate that cross validation is theoretically justified in choosing the tuning parameters for estimating the precision matrix.

In the present paper, we develop a simple column-wise procedure, called Sparse Column-wise Inverse Operator (SCIO), to study estimation of the precision matrix $\mathbf{\Omega}$. This procedure works for both sparse and non-sparse matrices without restricting to a specific sparsity pattern. We establish theoretical guarantees for the SCIO estimator. Rates of convergence in spectral norm as well as elementwise ℓ_∞ norm and Frobenius norm are established. A matrix is called s -sparse if there are at most s non-zero elements on each row. It is shown that when $\mathbf{\Omega}$ is s -sparse and \mathbf{X} has either exponential-type or polynomial-type

tails, the error between our estimator $\hat{\Omega}$ and Ω satisfies $\|\hat{\Omega} - \Omega\|_2 = O_P(s\sqrt{\log p/n})$ and $|\hat{\Omega} - \Omega|_\infty = O_P(\sqrt{\log p/n})$, where $\|\cdot\|_2$ and $|\cdot|_\infty$ are the spectral norm and elementwise l_∞ norm respectively. The SCIO method can also be adopted for the selection of graphical models (Lauritzen, 1996), where the elementwise l_∞ norm result is instrumental.

A significant advantage of the SCIO estimator is its computational efficiency for large-scale problems, thanks to its column-by-column computation. From a pure computational point of view, column-by-column procedures are examples of the general divide-and-conquer principal for large-scale computation. The estimator can be obtained one column at a time by solving a simple objective function for each column, and the resulting matrix estimator is formed by combining the vector solutions into a matrix. The final step is to symmetrize the matrix using a simple operation, which we used in Cai, Liu and Luo (2011). An improvement of computation comes from the key observation that the simple objective function for each column can be efficiently solved using the iterative coordinate descent algorithm, where each update is expressed in closed form. Indeed, this column-by-column computation principal has been employed for solving the ℓ_1 -MLE in its efficient R implementation *Glasso* by Friedman et al. (2008). However, they have two layers of iterations: one outer layer of iterations across the columns and an inner one to solve a LASSO problem iteratively using coordinate descent. The SCIO estimator no longer needs the outer iterations, and thus we observe improved computational speed in all of our examples. An R package of our method has been developed and is publicly available on CRAN.

The rest of the paper is organized as follows. In Section 2, after basic notations and definitions are introduced, we present the SCIO estimator. Theoretical properties including the rates of convergence are established in Section 3. A data-driven choice of the tuning parameter is discussed in Section 4, where we prove theoretical guarantees of using cross validation. The coordinate descent algorithm for solving SCIO is introduced in Section 5, and we also demonstrate its numerical performance through simulation studies and real data analyses. Further discussions on the connections and differences of our results with other related work are given in Section 6. The proofs of the main results are given in Section 7.

2 Methodology

In this section, we motivate the SCIO estimator. At the population level, given the population covariance matrix Σ , we define the column loss functions for every $i = 1, 2, \dots, p$,

which take the form

$$f_i(\boldsymbol{\Sigma}, \mathbf{B}) = \frac{1}{2} \boldsymbol{\beta}_i^T \boldsymbol{\Sigma} \boldsymbol{\beta}_i - \mathbf{e}_i^T \boldsymbol{\beta}_i \quad (1)$$

where $\mathbf{B} = (\boldsymbol{\beta}_1, \boldsymbol{\beta}_2, \dots, \boldsymbol{\beta}_p)$. Each function f_i in (1) is strictly convex in $\boldsymbol{\beta}_i$ as $\boldsymbol{\Sigma}$ is strictly positive-definite; more importantly, the minimal values of each f_i are achieved at $\boldsymbol{\beta}_i$'s that satisfy the following equality for each i

$$\boldsymbol{\Sigma} \boldsymbol{\beta}_i - \mathbf{e}_i = 0. \quad (2)$$

It is straightforward to see that the columns of the precision matrix $\boldsymbol{\Omega}$ satisfy these equalities, and thus minimize all the functions in (1). In fact, this is also the unique solution of (2) if $\boldsymbol{\Sigma}$ is full rank, given by the inversion formula $\boldsymbol{\omega}_i = \boldsymbol{\Sigma}^{-1} \mathbf{e}_i = \boldsymbol{\Omega} \mathbf{e}_i$.

Certainly, because $\boldsymbol{\Sigma}$ is usually unknown, the functions in the form (1) and the inversion formula cannot be directly applied to produce proper estimators of $\boldsymbol{\Omega}$. However, we can replace with the sample covariance matrix $\hat{\boldsymbol{\Sigma}}$ to produce the corresponding sample versions of (1):

$$f_i(\hat{\boldsymbol{\Sigma}}, \mathbf{B}) = \frac{1}{2} \boldsymbol{\beta}_i^T \hat{\boldsymbol{\Sigma}} \boldsymbol{\beta}_i - \mathbf{e}_i^T \boldsymbol{\beta}_i.$$

One intuitive idea is to minimize the above function to produce proper estimators for $\boldsymbol{\Omega}$. But this is not efficient because it does not utilize the assumption that the underlying $\boldsymbol{\Omega}$ is sparse, and more importantly there might be multiple solutions when $\hat{\boldsymbol{\Sigma}}$ is not full rank. This happens in high dimensional problems where p is much larger than n .

Motivated by recent developments on using the ℓ_1 norm to estimate the precision matrix (Friedman, Hastie, and Tibshirani, 2008; Cai, Liu and Luo, 2011), we use the ℓ_1 penalty to enforce the sparsity of each column-wise solution via minimizing the following objective function

$$\frac{1}{2} \boldsymbol{\beta}^T \hat{\boldsymbol{\Sigma}} \boldsymbol{\beta} - \mathbf{e}_i^T \boldsymbol{\beta} + \lambda_{ni} |\boldsymbol{\beta}|_1 \quad (3)$$

for each $i = 1, 2, \dots, p$, where the penalization parameter $\lambda_{ni} > 0$ can be different for different columns. By taking the subgradient of (3), the minimal values satisfy the following constraint for $i = 1, 2, \dots, p$,

$$\left| \hat{\boldsymbol{\Sigma}} \boldsymbol{\beta} - \mathbf{e}_i \right|_{\infty} \leq \lambda_{ni}.$$

This is exactly the constraint used for the CLIME estimator by Cai, Liu and Luo (2011).

We now proceed to formally define the SCIO estimator. Let $\hat{\boldsymbol{\beta}}_i$ be the solution to the following equation:

$$\hat{\boldsymbol{\beta}}_i = \arg \min_{\boldsymbol{\beta} \in \mathbb{R}^p} \left\{ \frac{1}{2} \boldsymbol{\beta}^T \hat{\boldsymbol{\Sigma}} \boldsymbol{\beta} - \mathbf{e}_i^T \boldsymbol{\beta} + \lambda_{ni} |\boldsymbol{\beta}|_1 \right\}, \quad (4)$$

where $\boldsymbol{\beta} = (\beta_1, \dots, \beta_p)^T$. The fully data-driven choice of λ_{ni} is introduced in Section 4. Let $\hat{\boldsymbol{\beta}}_i = (\hat{\beta}_{i1}, \dots, \hat{\beta}_{ip})^T$. Similar to the CLIME estimator, the solution of (4) is not necessarily symmetric. To obtain the SCIO estimator $\hat{\boldsymbol{\Omega}} = (\hat{\omega}_{ij})_{p \times p}$, we will employ the same symmetrization step as in CLIME,

$$\hat{\omega}_{ij} = \hat{\omega}_{ji} = \hat{\beta}_{ij} I\{|\hat{\beta}_{ij}| < |\hat{\beta}_{ji}|\} + \hat{\beta}_{ji} I\{|\hat{\beta}_{ij}| \geq |\hat{\beta}_{ji}|\}. \quad (5)$$

The choice of λ_{ni} , as will be given in Section 4, is adaptive to the columns of precision matrix. In real applications, the sparsity in each column may be different dramatically. The adaptive choice of the tuning parameter is chosen using our column-by-column loss. The Glasso estimator by Friedman, Hastie, and Tibshirani (2008), on the other hand, does not provide an inexpensive implementation like ours because they aim to compute the whole matrix using a likelihood loss of all entries, which consists of determinant computation for example.

3 Theoretical guarantees

In this section, we state the convergence rates of $\hat{\boldsymbol{\Omega}}$. The result on support recovery is also given. We begin with basic notations and definitions. Throughout, for a vector $\mathbf{a} = (a_1, \dots, a_p)^T \in \mathbb{R}^p$, define $\|\mathbf{a}\|_1 = \sum_{j=1}^p |a_j|$ and $\|\mathbf{a}\|_2 = \sqrt{\sum_{j=1}^p a_j^2}$. For a matrix $A = (a_{ij}) \in \mathbb{R}^{p \times q}$, we define the elementwise l_∞ norm $\|A\|_\infty = \max_{1 \leq i \leq p, 1 \leq j \leq q} |a_{i,j}|$, the spectral norm $\|A\|_2 = \sup_{\|\mathbf{x}\|_2 \leq 1} \|A\mathbf{x}\|_2$, the matrix l_1 norm $\|A\|_{L_1} = \max_{1 \leq j \leq q} \sum_{i=1}^p |a_{i,j}|$, the matrix ∞ norm $\|A\|_\infty = \max_{1 \leq i \leq q} \sum_{j=1}^p |a_{i,j}|$, the Frobenius norm $\|A\|_F = \sqrt{\sum_{i,j} a_{i,j}^2}$, and the elementwise l_1 norm $\|A\|_1 = \sum_{i=1}^p \sum_{j=1}^q |a_{i,j}|$. I denotes a $p \times p$ identity matrix. For any two index sets T and T' and matrix A , we use $A_{TT'}$ to denote the $|T| \times |T'|$ matrix with rows and columns of A indexed by T and T' respectively. The notation $A \succ 0$ means that A is positive definite. For two real sequences $\{a_n\}$ and $\{b_n\}$, write $a_n = O(b_n)$ if there exists a constant C such that $|a_n| \leq C|b_n|$ holds for large n , $a_n = o(b_n)$ if $\lim_{n \rightarrow \infty} a_n/b_n = 0$.

3.1 Convergence rates of $\hat{\boldsymbol{\Omega}} - \boldsymbol{\Omega}$

We first introduce some conditions. The first condition is on the sparsity of $\boldsymbol{\Omega}$. Let \mathcal{S}_i be the support of $\boldsymbol{\omega}_{\cdot,i}$, the i -th column in $\boldsymbol{\Omega}$. Define the s_p -sparse matrices class

$$\mathcal{U} = \left\{ \boldsymbol{\Omega} \succ 0 : \max_{1 \leq j \leq p} \sum_{i=j}^p I\{\omega_{ij} \neq 0\} \leq s_p, \quad \|\boldsymbol{\Omega}\|_{L_1} \leq M_p, \right. \\ \left. c_0^{-1} \leq \lambda_{\min}(\boldsymbol{\Omega}) \leq \lambda_{\max}(\boldsymbol{\Omega}) \leq c_0 \right\},$$

where c_0 is a positive constant.

(C1). Suppose that $\mathbf{\Omega} \in \mathcal{U}$ with

$$s_p = o\left(\sqrt{\frac{n}{\log p}}\right) \quad (6)$$

and

$$\max_{1 \leq i \leq p} \|\mathbf{\Sigma}_{\mathcal{S}_i^c \times \mathcal{S}_i} \mathbf{\Sigma}_{\mathcal{S}_i \times \mathcal{S}_i}^{-1}\|_\infty \leq 1 - \alpha \quad (7)$$

for some $0 < \alpha < 1$.

As we will see from Theorem 1, condition (6) is required for the consistency of the estimator. Condition (7) is a mutual incoherence or irrepresentable condition. Such a condition is almost necessary for support recovery through the penalization method. A similar irrepresentable condition was imposed by Ravikumar et al. (2011) for analyzing Glasso. We will compare (7) to their irrepresentable condition in Remark 3.

Let $\mathbf{Y} = (Y_1, \dots, Y_p)^T = \mathbf{\Omega}\mathbf{X} - \mathbf{\Omega}\boldsymbol{\mu}$. The covariance matrix of \mathbf{Y} is thus $\mathbf{\Omega}$. The second condition is on the moment of \mathbf{X} and \mathbf{Y} .

(C2). (Exponential-type tails) Suppose that $\log p = o(n)$. There exist positive numbers $\eta > 0$ and $K > 0$ such that

$$\mathbb{E} \exp\left(\eta(X_i - \mu_i)^2\right) \leq K, \quad \mathbb{E} \exp\left(\eta Y_i^2\right) \leq K \quad \text{for all } 1 \leq i \leq p.$$

(C2*). (Polynomial-type tails) Suppose that for some $\gamma, c_1 > 0$, $p \leq c_1 n^\gamma$, and for some $\delta > 0$

$$\mathbb{E}|X_i - \mu_i|^{4\gamma+4+\delta} \leq K, \quad \mathbb{E}|Y_i|^{4\gamma+4+\delta} \leq K \quad \text{for all } i.$$

We will assume either one of these two types of tails in our analysis. These two conditions are standard for analyzing precision matrix estimation, see Cai, Liu and Luo (2011) and references within.

The first result is on the convergence rate under the spectral norm. It implies the convergence rates of the estimation of eigenvalue and eigenvector, which is essential in principle component analysis. The convergence rate under spectral norm is also required in the classification problem, wherein the estimation of the precision matrix plays an important role.

Theorem 1 *Let $\lambda_{ni} = C_0 \sqrt{\log p/n}$ with C_0 being a sufficiently large number. Under (C1) and (C2) (or (C2*)), we have*

$$\|\hat{\mathbf{\Omega}} - \mathbf{\Omega}\|_2 \leq C_1 M_p s_p \sqrt{\frac{\log p}{n}}$$

with probability greater than $1 - O(p^{-1} + n^{-\delta/8})$, where $C_1 > 0$ depends only on c_0, η, C_0 and K .

Remark 1. If $M_p s_p \sqrt{\frac{\log p}{n}} = o(1)$, then $\hat{\Omega}$ is positive definite with probability tending to one. We can also revise $\hat{\Omega}$ to $\hat{\Omega}_\rho$ with

$$\hat{\Omega}_\rho = \hat{\Omega} + \rho \mathbf{I}, \quad (8)$$

where $\rho = (|\lambda_{\min}(\hat{\Omega})| + n^{-1/2}) I\{\lambda_{\min}(\hat{\Omega}) \leq 0\}$. Then $\hat{\Omega}$ is always positive definite. By Theorem 1, we have $\rho \leq C M_p s_p \sqrt{\frac{\log p}{n}}$ with probability greater than $1 - O(p^{-1} + n^{-\delta/8})$ and hence

$$\|\hat{\Omega}_\rho - \Omega\|_2 \leq C M_p s_p \sqrt{\frac{\log p}{n}}.$$

Such a simple perturbation will make the estimator be positive definite. The later results concerning support recovery and the convergence rates under other norms also hold under such a perturbation. To improve numerical stability, this perturbation strategy (8) can also be applied to the sample covariance as long as $\rho = O(n^{-1/2} \log^{1/2} p)$, and all the theoretical results also hold under such a perturbation, see also Cai, Liu and Luo (2011).

Remark 2. Ravikumar et al. (2011) imposed the following irrerepresentable condition on Glasso estimation: for some $0 < \alpha < 1$,

$$\max_{e \in S^c} |\mathbf{E}(\Phi_e \Phi_S^T) \mathbf{E}(\Phi_S \Phi_S^T)^{-1}|_1 \leq 1 - \alpha, \quad (9)$$

where S is the support of Ω and $\Phi_{(j,k)} = X_j X_k - \mathbf{E} X_j X_k$. To make things concrete, we now compare our conditions using the examples given in Ravikumar et al. (2011):

1. In the diamond graph, let $p = 4$, $\sigma_{ii} = 1$, $\sigma_{23} = 0$, $\sigma_{14} = 2\rho^2$ and $\sigma_{ij} = \rho$ for all $i \neq j$, $(i, j) \neq (2, 3)$ and $(2, 4)$. For this matrix, (9) is reduced to $4|\rho|(|\rho| + 1) < 1$ and so it requires $\rho \in (-0.208, 0.208)$. We prove that our condition (7) only needs $\rho \in (-0.5, 0.5)$.
2. In the star graph, let $p = 4$, $\sigma_{ii} = 1$, $\sigma_{1,j} = \rho$ for $j = 2, 3, 4$, $\sigma_{ij} = \rho^2$ for $1 < i < j \leq 4$. For this model, (12) requires $|\rho|(|\rho| + 2) < 1$ ($\rho \in (-0.4142, 0.4142)$), while our condition (7) holds for all $\rho \in (-1, 1)$.

We also have the following result on the convergence rates under the element-wise l_∞ norm and the Frobenius norm.

Theorem 2 Under the conditions of Theorem 1, we have with probability greater than $1 - O(p^{-1} + n^{-\delta/8})$,

$$|\hat{\Omega} - \Omega|_\infty \leq CM_p \sqrt{\frac{\log p}{n}} \quad (10)$$

and

$$\frac{1}{p} \|\hat{\Omega} - \Omega\|_F^2 \leq Cs_p \frac{\log p}{n}. \quad (11)$$

Remark 3. Note that the convergence rate under the Frobenius norm does not depend on M_p . On the other hand, Cai, Liu and Zhou (2011) obtained the minimax lower bound result when $\mathbf{X} \sim N(\boldsymbol{\mu}, \boldsymbol{\Sigma})$

$$\frac{1}{p} \min_{\hat{\Omega}} \max_{\Omega \in \mathcal{U}^*} \mathbb{E} \|\hat{\Omega} - \Omega\|_F^2 \geq cM_p^2 s_p \frac{\log p}{n}. \quad (12)$$

The rate in (11) is faster than the rate in (12) since we consider a smaller matrix class. In Ravikumar et al. (2011), they proved that the Glasso estimator $\hat{\Omega}_{Glasso}$ has the following convergence rate

$$\frac{1}{p} \|\hat{\Omega}_{Glasso} - \Omega\|_2^2 = O_P\left(\kappa_\Gamma^2 s_p \frac{\log p}{n}\right), \quad (13)$$

where $\kappa_\Gamma = \|\Gamma^{-1}\|_{L_1}$ and $\Gamma = (\boldsymbol{\Sigma} \otimes \boldsymbol{\Sigma})_{SS}$. Our convergence rate is faster than their rate in (13) if $\kappa_\Gamma \rightarrow \infty$.

3.2 Support recovery

As discussed in the introduction, the support recovery is related to the Gaussian graphical model selection. The support of Ω is also recovered by SCIO. Let $\Psi = \{(i, j) : \omega_{ij} \neq 0\}$ be the support of Ω . Let

$$\hat{\Psi} = \{(i, j) : \hat{\omega}_{ij} \neq 0\}.$$

The next theorem gives the result on support recovery.

Theorem 3 (i). Under the conditions of Theorem 1, we have $\hat{\Psi} \subseteq \Psi$ with probability greater than $1 - O(p^{-1} + n^{-\delta/8})$. (ii). Suppose that for a sufficiently large number $C > 0$,

$$\theta_p := \min_{(i,j) \in \Psi} |\omega_{ij}| \geq CM_p \sqrt{\frac{\log p}{n}}. \quad (14)$$

Under the conditions of Theorem 1, we have $\hat{\Psi} = \Psi$ with probability greater than $1 - O(p^{-1} + n^{-\delta/8})$.

4 Data-driven choice of λ_{ni}

This section introduces the procedure on the choice of the tuning parameter λ_{ni} . We consider the following cross validation (CV) method for the analysis, similar to Bickel and Levina (2008). Divide the sample $\{\mathbf{X}_k; 1 \leq k \leq n\}$ into two subsamples at random. Let n_1 and $n_2 = n - n_1$ be the two sample sizes for the random split satisfying $n_1 \asymp n_2 \asymp n$, and let $\hat{\Sigma}_1^v, \hat{\Sigma}_2^v$ be the two sample covariance matrices from the v th split, for $v = 1, \dots, H$, where H is a fixed integer. Let $\hat{\beta}_i^v(\lambda)$ be the estimator minimizing

$$\hat{R}(\lambda) = \frac{1}{H} \sum_{v=1}^H \left[\frac{1}{2} (\hat{\beta}_i^v(\lambda))^T \hat{\Sigma}_2^v \hat{\beta}_i^v(\lambda) - \mathbf{e}_i^T \hat{\beta}_i^v(\lambda) \right]. \quad (15)$$

For implementation purposes, we can divide an interval $(0, a]$ by $\lambda_1 < \dots < \lambda_N$, where $\lambda_i = \frac{i}{N}a$. The final tuning parameter is chosen by

$$\hat{\lambda}_i = \arg \min_{\{\lambda_j; 1 \leq j \leq N\}} \hat{R}(\lambda_j). \quad (16)$$

The choice of $\hat{\lambda}_i$ could be different for estimating different columns of the precision matrix. It is thus adaptive to the sparsity of each column, comparing with the standard Glasso estimator. The theoretical property of Glasso is hard to analyze under CV. For the estimation of the covariance matrix, Bickel and Levina (2008) obtained the convergence rate under the Frobenius norm for the threshold estimator of covariance matrix, where the threshold is based on partial samples. However, it had been an open problem on the convergence rate for estimating the precision matrix when the tuning parameter is chosen by CV. Our Theorem 4 solves this problem by showing that the estimator based on the partial samples and $\hat{\lambda}_i$ from (15) can attain the optimal rate under the Frobenius norm. For simplicity, we let $H = 1$ as in Bickel and Levina (2008). Let $\hat{\Omega}_1^1 := (\hat{\omega}_{ij1}^1) = (\hat{\beta}_1^1(\hat{\lambda}_1), \dots, \hat{\beta}_p^1(\hat{\lambda}_p))$ be the corresponding column solutions when the tuning parameters are chosen using (16) for each column. The matrix $\hat{\Omega}_1^1$ is symmetrized as before,

$$\hat{\omega}_{ij}^1 = \hat{\omega}_{ji}^1 = \hat{\omega}_{ij1}^1 I\{|\hat{\omega}_{ij1}^1| < |\hat{\omega}_{ji1}^1|\} + \hat{\omega}_{ji1}^1 I\{|\hat{\omega}_{ij1}^1| \geq |\hat{\omega}_{ji1}^1|\}.$$

The following theorem shows that the estimator $\hat{\Omega}^1 = (\hat{\omega}_{ij}^1)$ attains the optimal rate under the Frobenius norm.

Theorem 4 *Under the conditions of Theorem 1, $\log N = O(\log p)$, $\sqrt{n/\log p} = o(N)$ and $\mathbf{X} \sim N(\boldsymbol{\mu}, \boldsymbol{\Sigma})$, we have as $n, p \rightarrow \infty$,*

$$\frac{1}{p} \|\hat{\Omega}^1 - \boldsymbol{\Omega}\|_F^2 = O_P\left(s_p \frac{\log p}{n}\right).$$

Theorem 4 provides a parallel result to Bickel and Levina (2008)'s Theorem 4, where they obtained the same rate for estimating the covariance matrix under CV. Using similar arguments of theirs, this result can be extended to multiple folds. The assumption that $\mathbf{X} \sim N(\boldsymbol{\mu}, \boldsymbol{\Sigma})$ can be extended to the sub-Gaussian tails or the polynomial-type tails. The normality is only used for simplifying the proof. Theorem 4 is the first result on the convergence rate for estimating the precision matrix based on CV.

5 Numerical examples

We will first briefly introduce our algorithms for solving SCIO. We will then illustrate the numerical merits in estimation and computation using simulated and real datasets.

Recall the asymmetric estimator $\hat{\mathbf{B}} = (\hat{\boldsymbol{\beta}}_i)$ from (4), and the final SCIO estimator is obtained simply by applying symmetrization (5) to $\hat{\mathbf{B}}$. We compute each column $\hat{\boldsymbol{\beta}}_i$ by

$$\hat{\boldsymbol{\beta}}_i = \arg \min_{\boldsymbol{\beta}_i \in \mathbb{R}^p} \left\{ \frac{1}{2} \boldsymbol{\beta}_i^T \boldsymbol{\Sigma}_n \boldsymbol{\beta}_i - \boldsymbol{\beta}_i^T \mathbf{e}_i + \lambda \|\boldsymbol{\beta}_i\|_1 \right\}. \quad (17)$$

This objective can be solved easily using iterative coordinate descent. To simplify the notation, we will use $\boldsymbol{\beta}$ to denote $\boldsymbol{\beta}_i$ in (17) for a fixed i , as we will apply the same algorithm for each column i . In each iteration, we fix all but one coordinate in $\boldsymbol{\beta}$, and optimize over that coordinate. Without loss of generality, we consider optimizing over the p th coordinate β_p while all other coordinates of $\boldsymbol{\beta}$ (denoted by $\boldsymbol{\beta}_{-p}$) are fixed, the solution is given in explicit form by the following lemma. The solution for optimizing other coordinates while fixing the remaining ones are similar, simply by permuting the matrix to have that coordinate being the last one. We will iterate through coordinates until convergence.

Lemma 1 *Let the subvector partition $\boldsymbol{\beta} = (\boldsymbol{\beta}_{-p}, \beta_p)$ and partition $\boldsymbol{\Sigma}_n$ similarly as follows*

$$\boldsymbol{\Sigma}_n = \begin{pmatrix} \boldsymbol{\Sigma}_{11} & \boldsymbol{\Sigma}_{12} \\ \boldsymbol{\Sigma}_{12}^T & \boldsymbol{\Sigma}_{22} \end{pmatrix}.$$

Fixing $\boldsymbol{\beta}_{-p}$, the minimizer of (17) is given by

$$\beta_p = \mathcal{T}(1 \{p = i\} - \boldsymbol{\beta}_{-p}^T \boldsymbol{\Sigma}_{12}, \lambda) / \boldsymbol{\Sigma}_{22}$$

where the soft thresholding rule $\mathcal{T}(x, \lambda) = \text{sign}(x)(|x| - \lambda)$.

We implement this algorithm in an R package SCIO, and it is publicly available through CRAN. All the following numerical computation is performed using R on an AMD Opteron

processor (2.6 GHz) with 32 Gb memory. The Glasso estimator is computed using its R implementation *glasso* (version 1.7). We have also implemented the path-following strategies (Friedman et al 2008) in SCIO similar to the Glasso implementation, where the solutions are obtained in the decreasing order of λ 's and the initializer for each λ is set to the converged solution under its predecessor λ . We set the numerical accuracy to be 10^{-4} for both SCIO and Glasso, so that iterations stop in both algorithms when the changes are less than the accuracy.

5.1 Simulations

We compare the performance of our estimators with Glasso using simulations. The covariance matrix that we use to generate data contain two block diagonals, where the second block is 4 times the first one. Similar examples have been used in Cai and Liu (2011) in studying adaptive covariance estimation. The first block is generated from the following models respectively.

1. **decay**: $[\Omega_1^*]_{ij} = 0.6^{|i-j|}$.
2. **sparse**: Let $\Omega_0 = \mathbf{O} + \delta \mathbf{I}$, where each off-diagonal entry in \mathbf{O} is generated independently and equals to 0.5 with probability 0.1 or 0 with probability 0.9. δ is chosen such that the conditional number (the ratio of maximal and minimal singular values of a matrix) is equal to p . Finally, this matrix block is standardized to have unit diagonals.
3. **block**: A block diagonal matrix with block size 5 where each block has off-diagonal entries equal to 0.5 and diagonal 1. The resulting matrix is then randomly permuted.

For each model, 100 observations are generated from multivariate Gaussian distribution as a training data set, and 100 additional observations are generated from the same model as a validating data set. Using the training data, a series of estimators with 50 different values of λ are computed. For a fair comparison, we first pick the tuning parameters of Glasso and SCIO by minimizing the Bregman loss respectively on the validation sample. The Bregman loss is defined by

$$L(\Sigma, \Omega) = \langle \Omega, \Sigma \rangle - \log \det(\Omega).$$

We also compare with our theoretically justified CV scheme with the column-wise loss (15). The theoretical guarantee of this CV method is proved in Theorem 4. The resulting

estimator is denoted by SCIOcv. We consider different values of $p = 50, 100, 200, 400$ and replicate 100 times.

Table 1 compares the estimation performance of SCIO, SCIOcv, and Glasso under the spectral norm and the Frobenius norm. It shows that SCIO almost uniformly outperforms Glasso under both norms. The SCIO estimator shows slightly worse performance in the Block model but the difference is very small. The SCIOcv estimator is almost always the second best, probably because the Bregman loss is the correct likelihood criterion here.

The support of the inverse covariance matrix carries important consequences for the graphical models. The frequencies of correct zero/nonzero identification are summarized in Table 2. The true negative rates (TN%) shows that the SCIO estimates are sparser than Glasso estimates. To illustrate this, we plot the heatmaps of support recovery in Figure 1 using $p = 100$ as an representing example. These heatmaps confirm that our SCIO estimates are sparser than Glasso. By visual inspection, these SCIO estimates also tend to be closer to the truth. They are robust in these two-block models where the sparsity of the estimated two blocks are not interfered by their scale, whereas Glasso has shown some interference and artificial stripes appearing in the estimates under the Sparse model. The SCIOcv estimators almost always have the sparsity patterns between the SCIO and Glasso estimators.

5.2 HIV-1 associated neurocognitive disorders

Antiretroviral therapy (ART) has greatly reduced mortality and morbidity of HIV patients; however, HIV-1 associated neurocognitive disorders (HAND) are common among patients, which cause greatly degradation of life quality. Borjabad et al (2011) analyzed gene expression arrays on post-mortem brain tissues. They showed that patients with HAND on ART have many fewer and milder gene expression changes than untreated patients, and these genes are postulated to regulate certain pathways. The dataset is publicly available from Gene Expression Omnibus (GEO) under the serial number GSE28160. We here apply our graphical models to study how their genetic interactions/pathways are altered between treated and untreated patients, and compare with other methods on classification of future samples.

This dataset contains gene expression profiles of post-mortem brain tissues using two biological replications. The first replication dataset contains 6 control (healthy) samples, 7 treated HAND samples, and 8 untreated HAND samples; the second contains 3 controls, 5 treated, and 6 untreated. The data are preprocessed by GEO and then log-transformed using Bioconductor in R. We will use the first replications as a training set, and test the

Table 1: Comparison of average (SD) losses of SCIO, SCIOcv, and Glasso over 100 simulation runs. The best performance is highlighted in bold.

Spectral Norm									
p	Decay			Sparse			Block		
	SCIO	SCIOcv	Glasso	SCIO	SCIOcv	Glasso	SCIO	SCIOcv	Glasso
50	10.00(0.39)	11.24(0.28)	12.10(0.16)	2.73(0.43)	4.03(0.43)	3.86(0.25)	7.24(0.47)	9.55(0.16)	9.61(0.14)
100	11.89(0.20)	12.68(0.17)	13.11(0.11)	4.51(0.22)	5.57(0.21)	5.70(0.15)	9.63(0.21)	9.78(0.10)	9.77(0.09)
200	12.88(0.18)	13.46(0.10)	13.84(0.12)	7.93(0.14)	8.31(0.08)	8.48(0.09)	9.88(0.07)	9.85(0.06)	9.83(0.08)
400	13.63(0.12)	13.87(0.04)	14.07(0.03)	10.88(0.05)	11.60(0.04)	11.11(0.05)	9.92(0.07)	9.91(0.07)	9.87(0.07)

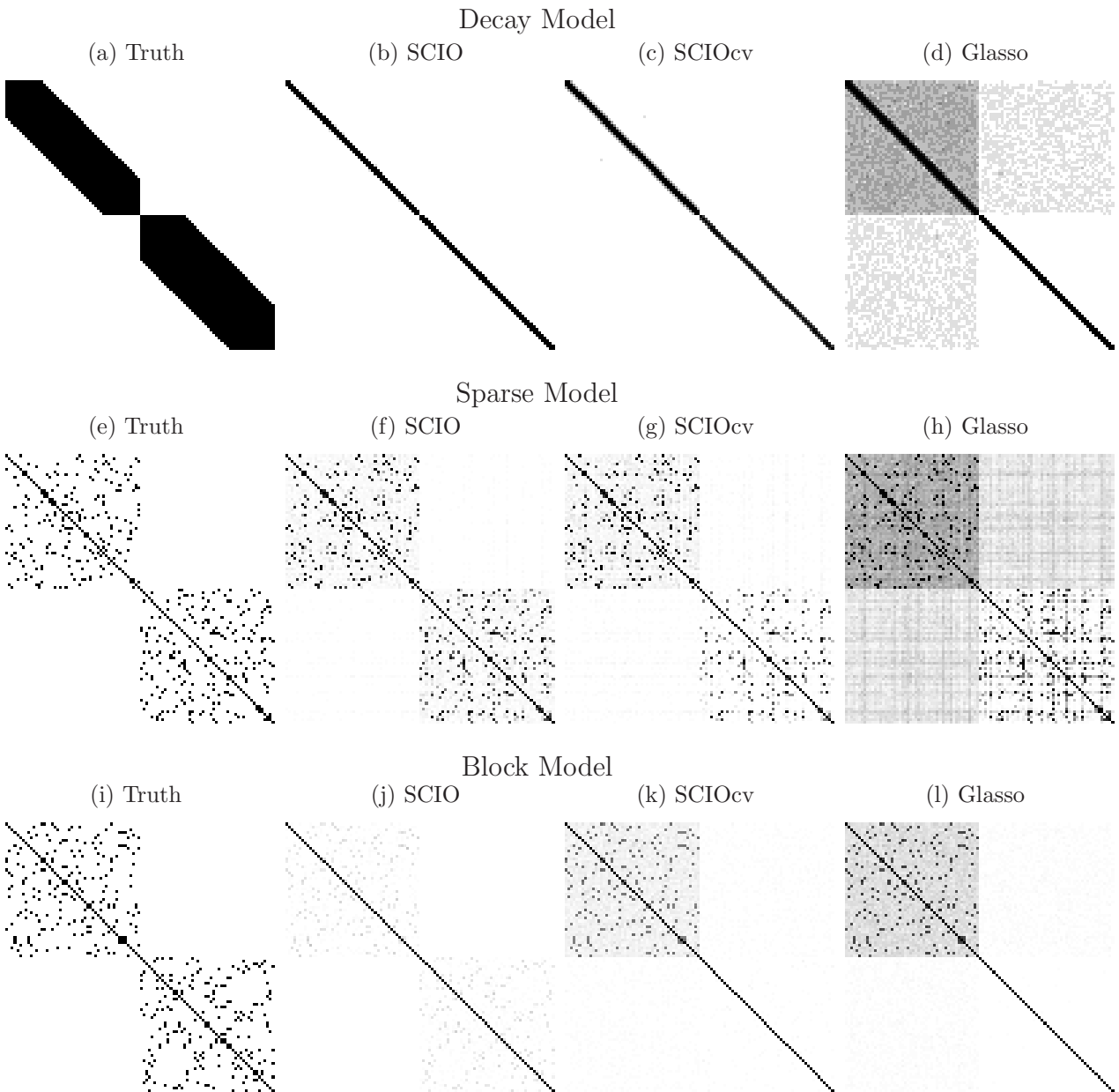
Frobenius Norm									
p	Decay			Sparse			Block		
	SCIO	SCIOcv	Glasso	SCIO	SCIOcv	Glasso	SCIO	SCIOcv	Glasso
50	16.22(0.66)	18.54(0.52)	20.18(0.37)	6.71(0.48)	7.95(0.52)	8.14(0.46)	16.10(1.01)	20.98(0.45)	21.68(0.29)
100	27.48(0.51)	29.58(0.44)	30.92(0.37)	12.93(0.37)	14.84(0.38)	14.91(0.37)	30.83(0.62)	31.02(0.15)	31.15(0.15)
200	42.93(0.74)	45.12(0.39)	47.00(0.64)	24.34(0.37)	24.67(0.23)	26.11(0.29)	44.49(0.12)	44.23(0.11)	44.19(0.12)
400	65.61(0.81)	66.60(0.24)	68.10(0.14)	36.65(0.26)	38.99(0.28)	37.76(0.28)	62.91(0.12)	62.73(0.12)	62.54(0.13)

Table 2: Comparison of average support recovery (SD) of SCIO, SCIOcv, and Glasso over 100 simulation runs.

TN%									
p	Decay			Sparse			Block		
	SCIO	SCIOcv	Glasso	SCIO	SCIOcv	Glasso	SCIO	SCIOcv	Glasso
50	98.57(0.72)	97.22(0.84)	76.18(3.06)	85.16(1.62)	97.73(0.54)	83.16(2.45)	80.60(1.93)	95.67(0.98)	87.40(5.12)
100	99.71(0.13)	98.97(0.21)	86.03(1.60)	91.40(0.44)	98.73(0.20)	86.69(1.16)	97.34(2.44)	98.69(0.32)	96.72(1.27)
200	99.98(0.02)	99.61(0.06)	94.97(2.20)	96.11(0.29)	99.42(0.07)	90.55(0.66)	99.97(0.12)	99.71(0.07)	99.03(0.36)
400	100.00(0.00)	99.84(0.02)	98.90(0.16)	98.66(0.06)	99.72(0.03)	95.60(0.44)	100.00(0.01)	99.94(0.01)	99.68(0.11)

TP%									
p	Decay			Sparse			Block		
	SCIO	SCIOcv	Glasso	SCIO	SCIOcv	Glasso	SCIO	SCIOcv	Glasso
50	24.19(2.24)	21.60(1.65)	35.92(2.32)	98.71(1.22)	93.27(2.75)	96.00(2.28)	95.18(2.83)	58.26(5.12)	62.45(6.20)
100	12.67(0.52)	13.77(0.76)	26.44(1.37)	77.73(2.12)	75.73(2.50)	83.55(2.66)	31.09(10.94)	41.94(3.33)	48.98(3.48)
200	10.14(0.26)	9.92(0.38)	16.15(3.46)	41.20(1.68)	29.78(1.33)	62.98(1.73)	20.02(0.11)	30.11(1.70)	38.81(3.11)
400	7.14(0.78)	7.84(0.18)	8.81(0.37)	10.68(0.39)	12.03(0.44)	33.83(1.41)	20.00(0.01)	24.63(0.75)	32.15(2.02)

Figure 1: Heatmaps of support recovery over 100 simulation runs (black is 100/100, white is 0/100).



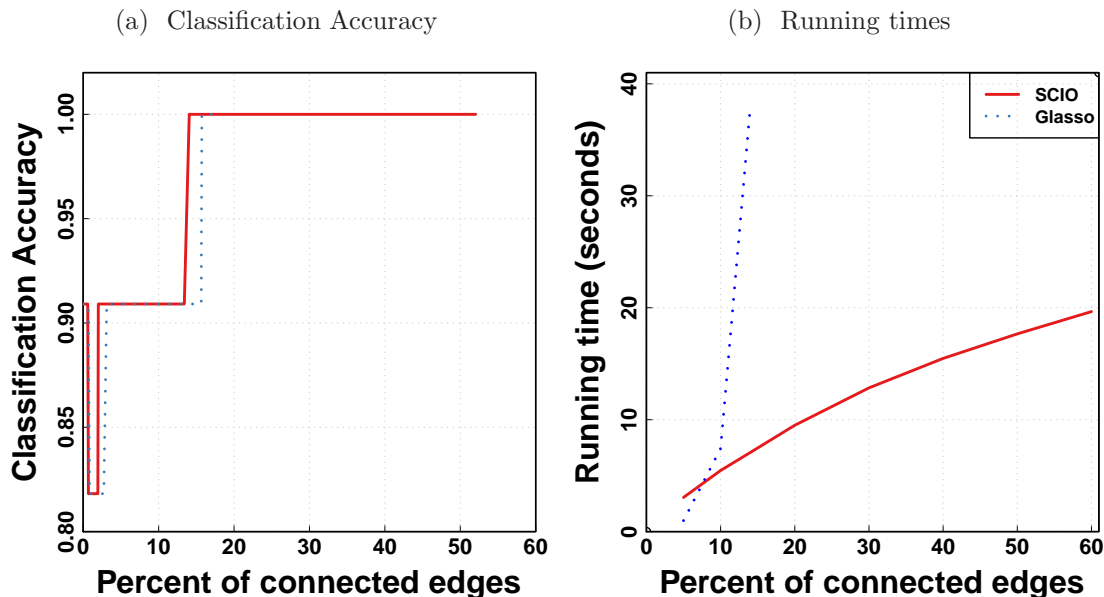
classification performance of 3 classes on the second replications. The class label is denoted by k , where $k=1,2,3$ for control, treated and untreated respectively. The model building procedure is similar to our previous paper Cai, Liu and Luo (2011). On the training data, we first compare pair-wise mean differences between 3 classes for each gene using Wilcoxon’s test, and select the top 100 genes with the most significant p-values in any of the tests. Based on these 100 genes and the training data, we estimate the inverse covariance matrix $\hat{\Omega}_k$ for each class k using SCIO and Glasso. For a new observation X from the testing dataset, the classification score for each pair of class (k, k') is by the log-likelihood difference (ignoring constant factors)

$$s_{k,k'}(X) = - (X - \bar{X}_k) \hat{\Omega}_k (X - \bar{X}_k) + (X - \bar{X}_{k'}) \hat{\Omega}_{k'} (X - \bar{X}_{k'}) \\ + \log \det \left(\hat{\Omega}_k \right) - \log \det \left(\hat{\Omega}_{k'} \right)$$

where \bar{X}_l is the mean vector for class l using the training data, $l = k, k'$ and $k \neq k'$. This score is essentially the log-likelihood differences under two estimated multivariate normal distributions. Because each class has almost the same number of observations in the training data, we will assign the label k if $s_{k,k'} > 0$ and k' otherwise.

Figure 2a compares classification accuracy of treated and untreated HAND using SCIO and Glasso. The results comparing two HAND groups with the controls respectively are not shown because we have constant area-under-the-curve values equal to 1 in both comparisons. Because the number of nonzero off-diagonal elements depends on the choice of penalization parameters in each method, we plot the classification accuracy against the average percentages of nonzero off-diagonals (or connected edges) of these two classes (treated and untreated) under each λ . The SCIOcv estimator (not shown) only differs from SCIO by the choice of picking λ , and it is irrelevant here as we show the performance across all λ 's. This figure shows that Glasso and SCIO have similar performance under most of the sparsity percentages, but SCIO outperforms Glasso using the same number of connected edges in some cases. The SCIO estimators have also stable classification performance even if the number of connected edges increases. We didn’t plot the performance of Glasso with more than 14% connected edges (smaller penalization parameters), because we found the Glasso algorithm didn’t converge within 120 hours to achieve the same sparsity percentages on the same dataset. As a side comparison with other classification algorithms, we build other classifiers using the same selected 100 genes from the training data, including random forest (Breiman, 2001), AIC penalized logistic regression, and L1 penalized logistic regression with 5-fold cross validated penalization parameters. Their classification accuracies are 78.6%, 90.9% and 45.6% respectively. Our classification rule compares favorably as well

Figure 2: Comparison of classification accuracy and running times using SCIO and Glasso for the HIV dataset. Red solid line is SCIO and blue dotted line is Glasso.

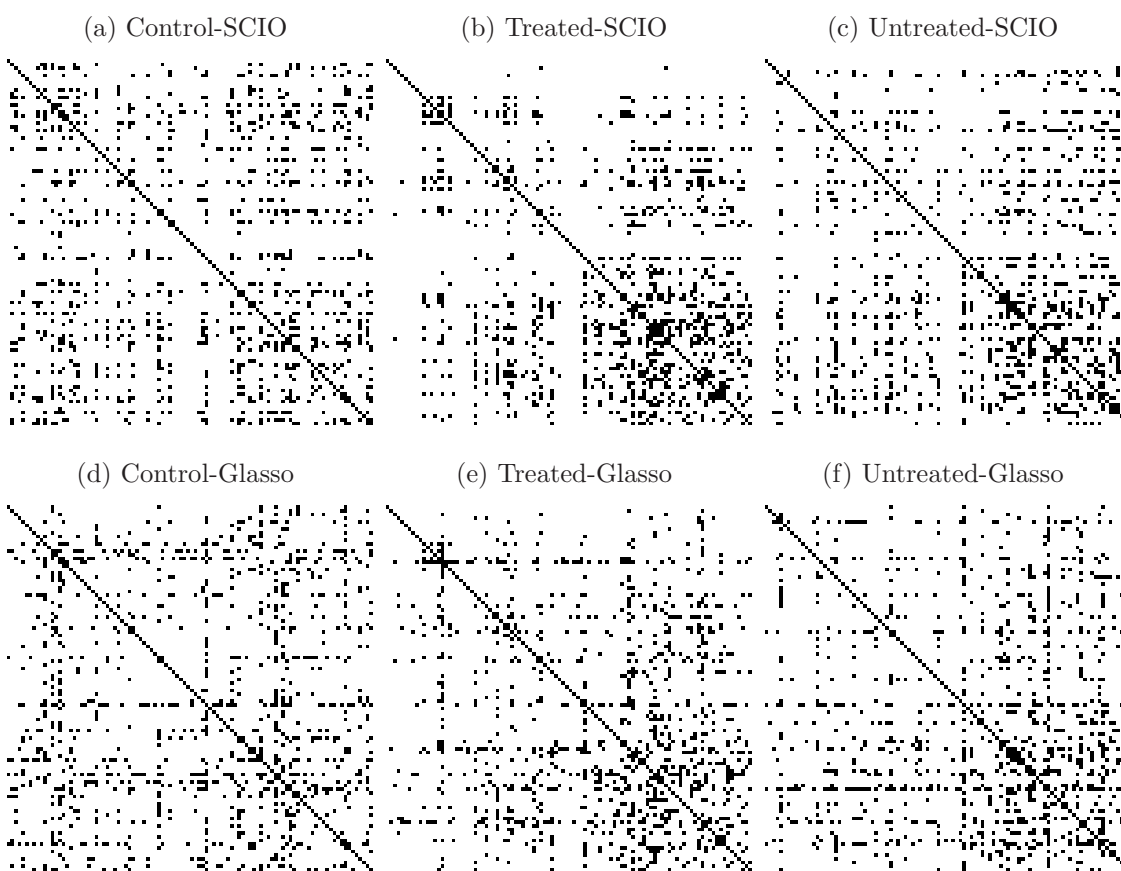


with these competing methods on this dataset.

To compare the computation time, Figure 2b plots the running times of Glasso and SCIO against the percentages of connected edges for the same reason as before. Because Friedman et al (2008b) showed that path-following algorithms compute a sequence of penalization parameters to a small value much faster than computing for the single small value, we use 50 log-spaced penalization parameters in each computation. They range from the largest (0% edges) to the values corresponding to the designated percentages of edges, including 5%, 10%, 14%, 20%, 30%, 40%, 50% and 60%. As reported before, we didn't plot the running times for Glasso beyond 14% because it didn't converge. SCIO takes about 2 seconds more than Glasso when computing for 5% edges, but is much faster than Glasso for 10% and more edges. It compares favorably in the 14% case where SCIO takes only a quarter of the time of Glasso. The running time of the SCIO estimator grows linearly with the number of connected edges, while Glasso has shown an exponential growth in time.

To compare the graphical models recovered, Figure 3 plots the supports with a representing case of 10% connected edges using both SCIO and Glasso. Each subject class has different connection patterns as shown by both SCIO and Glasso, and both methods also recover some shared patterns for each class. However, it is noted that Glasso tends to have artificial stripes in the pattern, which is also observed in simulations.

Figure 3: Comparison of support recovered by SCIO and Glasso for the HIV dataset, when we 10% of the edges are connected in all plots.



5.3 Attention deficit hyperactivity disorder

Attention Deficit Hyperactivity Disorder (ADHD) has substantial impairment among about 10% of school-age children in United States. Dickstein et al (2011) used resting state fMRI scans to show that there are differences in correlations between brain region among typically developed children and children with such disorders. The ADHD-200 project (http://fcon_1000.projects.nitrc.org/indi/adhd200/) released fMRI resting data of healthy control and ADHD children to encourage research on these diseases. We apply our method using the preprocessed data from neurobureau (<http://www.nitrc.org/plugins/mwiki/index.php/neurobureau>) from one of the participating center, Kennedy Krieger Institute. There are 61 typically-developing controls (HC), and 22 ADHD cases. The preprocessing steps are described in the same website. After preprocessing, we have 148 time points from each of 116 brain regions of each subject. We here want to study the precision matrix pattern for each subject, as it reveals conditional independence and is more relevant to explore direct connectivity.

We estimate the inverse covariance matrices using SCIO and Glasso with varying penalty parameters for each subject. As reported before, the connection patterns depend on the choice of penalty, and we thus compare patterns with the same percentage of connections for each subject. Figure 4 illustrates the average heatmaps across subjects of ADHD and HC respectively recovered by SCIO and Glasso. We let all individual precision matrices to have 30% connected edges as a representing case. Both methods have shown that ADHD has increased number of nonzero entries off the diagonal comparing with HC. Both methods recover similar patterns of nonzero entries close the diagonal, but SCIO tends to be less noisy on the entries far away from the diagonals.

The running times for both methods are compared in Figure 5. As reported before, for each subject, we use path following algorithms in both methods to designated connected edges, including 10%, 20%, 30%, 40%, 50% and 60%. We then plot the average running times and standard errors. This plot shows that the running times of SCIO grows almost linearly. Comparing with Glasso, SCIO is about 2 times faster with 60% connected edges.

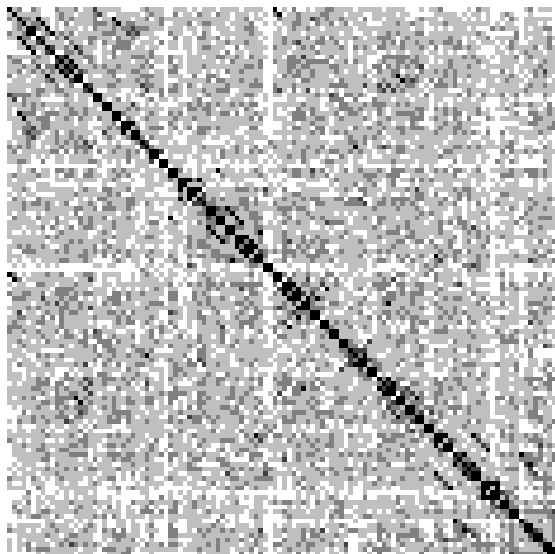
6 Discussion

We introduce the SCIO estimator in this paper. Theoretical guarantees of this estimator are established under various norms. We present a path-following algorithm for computing this estimator fast. The advantages of our estimators are also illustrated using both simulated and real examples.

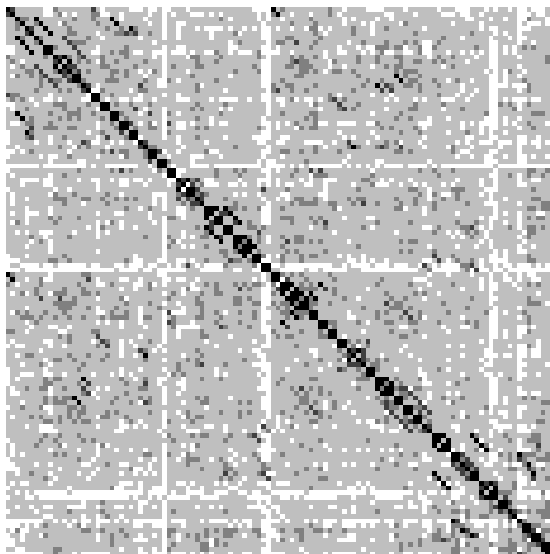
The choice of the tuning parameter is an important problem in applying penalization

Figure 4: Heatmaps of support recovered by SCIO and Glasso for the ADHD dataset, when we set 30% of the edges are connected in each subject.

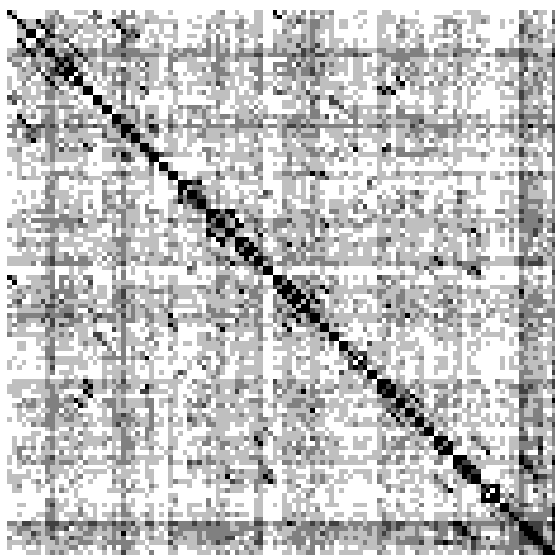
(a) ADHD-SCIO



(b) Control-SCIO



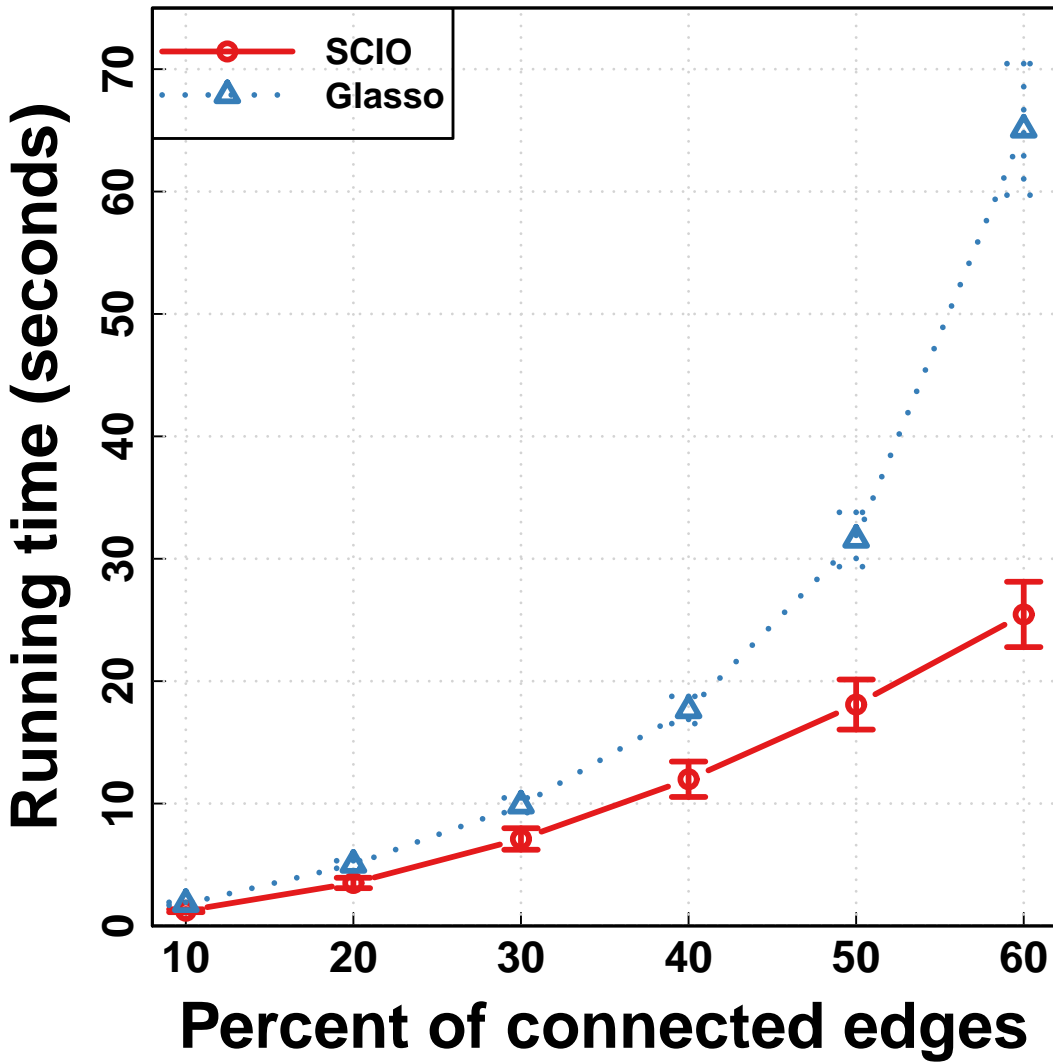
(c) ADHD-Glasso



(d) Control-Glasso



Figure 5: Comparison of average running times for the ADHD dataset.



procedures, despite numerous theoretical results. This paper is among the first to demonstrate that cross validation provides theoretical guarantees that the resulting estimator achieves the $n^{-1/2}(\log p)^{1/2}$ rate under the Frobenius norm. This rate may not be improved as we suspect it should be the minimax optimal rate. Moreover, it is very interesting to study whether such rate can also be achieved in other matrix norms, such as the operator norm, using data-driven choice of λ . These results will further bridge the gap between theory and practice of these penalization methods.

The rate we provide in Theorem 3 coincides with the minimax optimal rate in Cai, Liu and Zhou (2011). However, note that \mathcal{U} together with (7) is actually a smaller class of matrices than theirs. It is interesting to explore if their minimax rate can be improved in this important sub-class, though the current rate is already the desirable rate in high dimensional inference in general.

Penalized regression and inverse covariance estimation are closely connected problems in statistics. During the preparation of this paper, It comes to our attention that Sun and Zhang (2012) recently applied their recently developed penalized regression procedure, Scale Lasso, to the inverse covariance matrix estimation. Their procedure is aiming to adapt to the variances of the errors in regression. It is interesting to study if their procedure can also be applied under our column loss.

We considered enforcing sparsity via the ℓ_1 norm due to computational concerns. It has been pointed by several authors that the ℓ_1 penalty inheritably introduces biases in estimation, and thus it is interesting to replace the ℓ_1 norm by other penalty forms, such as Adaptive Lasso (Zou, 2006) or SCAD (Fan et al, 2009, Zhou et al, 2009). Such extensions should be easy to implement because our procedure only employs column-wise operations. We are currently implementing these methods for future releases of our R package.

There are other interesting directions to expand the current models. It is interesting to study precision matrix estimation when the data are generated from some hidden factor models, where the covariance estimation problem was studied by Luo (2011). Recently, Guo et al (2011) introduced a new penalty to jointly estimate multiple graphical models, assuming that these graphs have some shared patterns. It is interesting to extend our approach to that setting. It is also interesting to consider extending SCIO to the nonparanomral case for high dimensional undirected graphs (Liu et al, 2009).

This paper only considers the setting that all the data are observed. It is an interesting problem to study the inverse covariance matrix estimation when some of the data are possibly missing. It turns out that the SCIO procedure can also be applied to the missing data setting, with some modifications. Due to the space limitation, we will report these

results elsewhere.

7 Proof of main results

To prove the main results, we need the following lemma which comes from (28) in Cai, Liu and Luo (2011).

Lemma 1 *Under (C2) or (C2*), we have for some $C > 0$,*

$$P\left(\max_{1 \leq i, j \leq p} \{|\hat{\sigma}_{ij} - \sigma_{ij}| / (\sigma_{ii}^{1/2} \sigma_{jj}^{1/2})\} \geq C \sqrt{\frac{\log p}{n}}\right) = O(p^{-1} + n^{-\delta/8}).$$

Let $\boldsymbol{\Omega} = (\omega_{ij}) = (\boldsymbol{\omega}_1, \dots, \boldsymbol{\omega}_p)$, \mathcal{S}_i be the support of $\boldsymbol{\omega}_i$ and $\boldsymbol{\omega}_{\mathcal{S}_i} = (\omega_{ji}; j \in \mathcal{S}_i)^T$. The following lemma comes from Cai, Liu and Zhou (2011).

Lemma 2 *Under (C2) or (C2*) and $c_0^{-1} \leq \lambda_{\min}(\boldsymbol{\Omega}) \leq \lambda_{\max}(\boldsymbol{\Omega}) \leq c_0$, we have for some $C > 0$,*

$$P\left(\max_{1 \leq i \leq p} |\hat{\boldsymbol{\Sigma}}_{\mathcal{S}_i \times \mathcal{S}_i} \boldsymbol{\omega}_{\mathcal{S}_i} - \mathbf{e}_{\mathcal{S}_i}|_{\infty} \geq C \sqrt{\frac{\log p}{n}}\right) = O(p^{-1} + n^{-\delta/8}).$$

Proof of Theorem 1. For the solution $\hat{\boldsymbol{\beta}}_i$, it satisfies that

$$\hat{\boldsymbol{\Sigma}} \hat{\boldsymbol{\beta}}_i - \mathbf{e}_i = -\lambda_n \hat{\mathbf{Z}}_i,$$

where $\hat{\mathbf{Z}}_i = (\hat{Z}_{1i}, \dots, \hat{Z}_{pi})^T$ is the subdifferential $\partial|\hat{\boldsymbol{\beta}}_i|_1$ satisfying

$$\hat{Z}_{ji} = \begin{cases} 1, & \hat{\boldsymbol{\beta}}_{ji} > 0; \\ -1, & \hat{\boldsymbol{\beta}}_{ji} < 0; \\ \in [-1, 1], & \hat{\boldsymbol{\beta}}_{ji} = 0. \end{cases}$$

Define $\hat{\boldsymbol{\beta}}_i^o$ be the solution of the following optimization problem:

$$\hat{\boldsymbol{\beta}}_i^o = \arg \min_{\text{supp}(\boldsymbol{\beta}) \subseteq \mathcal{S}_i} \left\{ \frac{1}{2} \boldsymbol{\beta}^T \hat{\boldsymbol{\Sigma}} \boldsymbol{\beta} - \mathbf{e}_i^T \boldsymbol{\beta} + \lambda_n |\boldsymbol{\beta}|_1 \right\},$$

where $\text{supp}(\boldsymbol{\beta})$ denotes the support of $\boldsymbol{\beta}$. We will show that $\hat{\boldsymbol{\beta}}_i = \hat{\boldsymbol{\beta}}_i^o$ with probability greater than $1 - O(p^{-1} + n^{-\delta/8})$, and hence Theorem 1 can be obtained from Theorem 2.

Let $\hat{\mathbf{Z}}_{\mathcal{S}_i}^o$ is the subdifferential $\partial|\hat{\boldsymbol{\beta}}_i^o|_1$ on \mathcal{S}_i . We define the vector $\tilde{\mathbf{Z}}_i = (\tilde{Z}_{1i}, \dots, \tilde{Z}_{pi})^T$ by letting $\tilde{Z}_{ji} = \hat{Z}_{ji}^o$ for $j \in \mathcal{S}_i$ and

$$\tilde{Z}_{ji} = -\lambda_n^{-1} (\hat{\boldsymbol{\Sigma}} \hat{\boldsymbol{\beta}}_i^o)_j \quad \text{for } j \in \mathcal{S}_i^c.$$

By Lemma 3, for $j \in \mathcal{S}_i^c$ and some $r < 1$,

$$|\tilde{Z}_{ji}| \leq r < 1 \quad (18)$$

with probability greater than $1 - O(p^{-1} + n^{-\delta/8})$. By this primal-dual witness construction and (22), the theorem is proved. ■

Lemma 3 *With probability greater than $1 - O(p^{-1})$, we have*

$$|\tilde{Z}_{ji}| < 1 - \alpha/2$$

uniformly for $j \in \mathcal{S}_i^c$.

Proof. By the definition of $\tilde{\mathbf{Z}}_i$, we have

$$\hat{\Sigma}_{\mathcal{S}_i \times \mathcal{S}_i} \hat{\beta}_{\mathcal{S}_i}^o - \mathbf{e}_{\mathcal{S}_i} = -\lambda_n \tilde{\mathbf{Z}}_{\mathcal{S}_i} \quad (19)$$

and

$$\hat{\Sigma}_{\mathcal{S}_i^c \times \mathcal{S}_i} \hat{\beta}_{\mathcal{S}_i}^o = -\lambda_n \tilde{\mathbf{Z}}_{\mathcal{S}_i^c}. \quad (20)$$

Write (19) as

$$\Sigma_{\mathcal{S}_i \times \mathcal{S}_i} (\hat{\beta}_{\mathcal{S}_i}^o - \boldsymbol{\omega}_{\mathcal{S}_i}) + (\hat{\Sigma}_{\mathcal{S}_i \times \mathcal{S}_i} - \Sigma_{\mathcal{S}_i \times \mathcal{S}_i}) (\hat{\beta}_{\mathcal{S}_i}^o - \boldsymbol{\omega}_{\mathcal{S}_i}) + \hat{\Sigma}_{\mathcal{S}_i \times \mathcal{S}_i} \boldsymbol{\omega}_{\mathcal{S}_i} - \mathbf{e}_{\mathcal{S}_i} = -\lambda_n \tilde{\mathbf{Z}}_{\mathcal{S}_i}.$$

This implies that

$$\hat{\beta}_{\mathcal{S}_i}^o - \boldsymbol{\omega}_{\mathcal{S}_i} = \Sigma_{\mathcal{S}_i \times \mathcal{S}_i}^{-1} \left(-\lambda_n \tilde{\mathbf{Z}}_{\mathcal{S}_i} - (\hat{\Sigma}_{\mathcal{S}_i \times \mathcal{S}_i} - \Sigma_{\mathcal{S}_i \times \mathcal{S}_i}) (\hat{\beta}_{\mathcal{S}_i}^o - \boldsymbol{\omega}_{\mathcal{S}_i}) - \hat{\Sigma}_{\mathcal{S}_i \times \mathcal{S}_i} \boldsymbol{\omega}_{\mathcal{S}_i} + \mathbf{e}_{\mathcal{S}_i} \right). \quad (21)$$

By (6), Lemma 1 and Lemma 2, we have with probability greater than $1 - O(p^{-1} + n^{-\delta/8})$,

$$|\hat{\beta}_{\mathcal{S}_i}^o - \boldsymbol{\omega}_{\mathcal{S}_i}|_2 \leq C \sqrt{s_p \log p/n} + o(1) |\hat{\beta}_{\mathcal{S}_i}^o - \boldsymbol{\omega}_{\mathcal{S}_i}|_2.$$

This implies that

$$|\hat{\beta}_{\mathcal{S}_i}^o - \boldsymbol{\omega}_{\mathcal{S}_i}|_2 \leq C \sqrt{s_p \log p/n}. \quad (22)$$

By (20) and the above equation, we have

$$\begin{aligned} -\tilde{\mathbf{Z}}_{\mathcal{S}_i^c} &= \frac{1}{\lambda_n} \hat{\Sigma}_{\mathcal{S}_i^c \times \mathcal{S}_i} (\hat{\beta}_{\mathcal{S}_i}^o - \boldsymbol{\omega}_{\mathcal{S}_i}) + \frac{1}{\lambda_n} (\hat{\Sigma}_{\mathcal{S}_i^c \times \mathcal{S}_i} - \Sigma_{\mathcal{S}_i^c \times \mathcal{S}_i}) \boldsymbol{\omega}_{\mathcal{S}_i} \\ &= \frac{1}{\lambda_n} (\hat{\Sigma}_{\mathcal{S}_i^c \times \mathcal{S}_i} - \Sigma_{\mathcal{S}_i^c \times \mathcal{S}_i}) (\hat{\beta}_{\mathcal{S}_i}^o - \boldsymbol{\omega}_{\mathcal{S}_i}) - \Sigma_{\mathcal{S}_i^c \times \mathcal{S}_i} \Sigma_{\mathcal{S}_i \times \mathcal{S}_i}^{-1} \tilde{\mathbf{Z}}_{\mathcal{S}_i} \\ &\quad - \frac{1}{\lambda_n} \Sigma_{\mathcal{S}_i^c \times \mathcal{S}_i} \Sigma_{\mathcal{S}_i \times \mathcal{S}_i}^{-1} (\hat{\Sigma}_{\mathcal{S}_i \times \mathcal{S}_i} - \Sigma_{\mathcal{S}_i \times \mathcal{S}_i}) (\hat{\beta}_{\mathcal{S}_i}^o - \boldsymbol{\omega}_{\mathcal{S}_i}) \\ &\quad - \frac{1}{\lambda_n} \Sigma_{\mathcal{S}_i^c \times \mathcal{S}_i} \Sigma_{\mathcal{S}_i \times \mathcal{S}_i}^{-1} (\hat{\Sigma}_{\mathcal{S}_i \times \mathcal{S}_i} \boldsymbol{\omega}_{\mathcal{S}_i} - \mathbf{e}_{\mathcal{S}_i}) \\ &\quad + \frac{1}{\lambda_n} (\hat{\Sigma}_{\mathcal{S}_i^c \times \mathcal{S}_i} - \Sigma_{\mathcal{S}_i^c \times \mathcal{S}_i}) \boldsymbol{\omega}_{\mathcal{S}_i}. \end{aligned}$$

Since $\|\Sigma_{S_i^c \times S_i} \Sigma_{S_i \times S_i}^{-1}\|_\infty \leq 1 - \alpha$ and $|\tilde{\mathbf{Z}}_{S_i}|_\infty \leq 1$, we have $|\Sigma_{S_i^c \times S_i} \Sigma_{S_i \times S_i}^{-1} \tilde{\mathbf{Z}}_{S_i}|_\infty \leq 1 - \alpha$. By (22) and Lemma 1, we obtain that with probability greater than $1 - O(p^{-1} + n^{-\delta/8})$,

$$|(\hat{\Sigma}_{S_i^c \times S_i} - \Sigma_{S_i^c \times S_i})(\hat{\beta}_{S_i}^o - \omega_{S_i})|_\infty \leq C s_p \log p / n. \quad (23)$$

This, together with Lemma 2, implies (18). \blacksquare

Proof of Theorems 2 and 3. By the proof of Theorem 1, we have $\hat{\beta}_i = \hat{\beta}_i^o$. Note that

$$\hat{\beta}_i - \omega_i = \Sigma^{-1} \left(-\lambda_n \hat{\mathbf{Z}}_i - (\hat{\Sigma} - \Sigma)(\hat{\beta}_i - \omega_i) - \hat{\Sigma} \omega_i + \mathbf{e}_i \right). \quad (24)$$

By (22) and Lemma 1, we obtain that with probability greater than $1 - O(p^{-1} + n^{-\delta/8})$,

$$|(\hat{\Sigma} - \Sigma)(\hat{\beta}_i - \omega_i)|_\infty \leq C s_p \log p / n. \quad (25)$$

Thus,

$$|\hat{\beta}_i - \omega_i|_\infty \leq C M_p \sqrt{\frac{\log p}{n}}.$$

This proves (10). By (22) and the inequality $\|\hat{\Omega} - \Omega\|_F^2 \leq 2 \sum_{j=1}^p |\hat{\beta}_j - \omega_j|_2^2$, we obtain (11). Theorem 3 (i) follows from the proof of Theorem 1. Theorem 3 (ii) follows from Theorem 2 and the lower bound condition on θ_p . \blacksquare

Proof of Theorem 4. Let

$$\hat{\beta}_i^o = \arg \min_{\beta \in \mathbb{R}^p} \left\{ \frac{1}{2} \beta^T \hat{\Sigma}_1^1 \beta - \mathbf{e}_i^T \beta + \lambda |\beta|_1 \right\}$$

with $\lambda = C \sqrt{\log p / n} \in \{\lambda_i, 1 \leq i \leq N\}$ and C is sufficiently large. Then by the proofs of Theorem 1 and 2, we have with probability greater than $1 - O(p^{-1})$,

$$\max_{1 \leq i \leq p} |\hat{\beta}_i^o - \omega_i|_2^2 \leq C s_p \frac{\log p}{n}.$$

By the definition of $\hat{\beta}_i^1$, we have

$$\frac{1}{2} (\hat{\beta}_i^1)^T \hat{\Sigma}_2^1 \hat{\beta}_i^1 - \mathbf{e}_i^T \hat{\beta}_i^1 \leq \frac{1}{2} (\hat{\beta}_i^o)^T \hat{\Sigma}_2^1 \hat{\beta}_i^o - \mathbf{e}_i^T \hat{\beta}_i^o.$$

Set $\mathbf{D}_i = \hat{\beta}_i^1 - \omega_i$ and $\mathbf{D}_i^o = \hat{\beta}_i^o - \omega_i$. This implies that

$$\begin{aligned} & \langle (\hat{\Sigma}_2^1 - \Sigma) \mathbf{D}_i, \mathbf{D}_i \rangle + \langle \Sigma \mathbf{D}_i, \mathbf{D}_i \rangle + 2 \langle \hat{\Sigma}_2^1 \omega_i - \mathbf{e}_i, \hat{\beta}_i^1 - \hat{\beta}_i^o \rangle \\ & \leq \langle (\hat{\Sigma}_2^1 - \Sigma) \mathbf{D}_i^o, \mathbf{D}_i^o \rangle + \langle \Sigma \mathbf{D}_i^o, \mathbf{D}_i^o \rangle. \end{aligned}$$

We have by Lemma 4,

$$|\langle (\hat{\Sigma}_2^1 - \Sigma) \mathbf{D}_i, \mathbf{D}_i \rangle| = O_P(1) |\mathbf{D}_i|_2^2 \sqrt{\frac{\log N}{n}}$$

and

$$\langle \hat{\Sigma}_2^1 \boldsymbol{\omega}_i - \mathbf{e}_i, \hat{\boldsymbol{\beta}}_i^1 - \hat{\boldsymbol{\beta}}_i^o \rangle = O_P(1) |\hat{\boldsymbol{\beta}}_i^1 - \hat{\boldsymbol{\beta}}_i^o|_2 \sqrt{\frac{\log N}{n}}.$$

Thus,

$$|\mathbf{D}_i|_2^2 \leq O_P\left(\sqrt{\frac{\log N}{n}}\right) (|\mathbf{D}_i|_2 + |\hat{\boldsymbol{\beta}}_i^o - \boldsymbol{\omega}_i|_2) + |\mathbf{D}_i^o|_2^2.$$

This proves the theorem.

Lemma 4 For any vector \mathbf{v}_i with $|\mathbf{v}_i|_2 = 1$, we have

$$\max_{1 \leq i \leq N} |\langle (\hat{\Sigma}_2^1 - \Sigma) \mathbf{v}_i, \mathbf{v}_i \rangle| = O_P\left(\sqrt{\frac{\log N}{n}}\right) \quad (26)$$

and

$$\max_{1 \leq i \leq N} |\langle \hat{\Sigma}_2^1 \boldsymbol{\omega}_i - \mathbf{e}_i, \mathbf{v}_i \rangle| = O_P\left(\sqrt{\frac{\log N}{n}}\right). \quad (27)$$

Proof of Lemma 4. Note that

$$\langle (\hat{\Sigma}_2^1 - \Sigma) \mathbf{v}_i, \mathbf{v}_i \rangle = \langle (\Sigma^{-1/2} \hat{\Sigma}_2^1 \Sigma^{-1/2} - \mathbf{I}) \Sigma^{1/2} \mathbf{v}_i, \Sigma^{1/2} \mathbf{v}_i \rangle.$$

To prove (26), without loss of generality, we assume that $\Sigma = \mathbf{I}$. Then $\hat{\Sigma}_2^1$ has the same distribution as $\frac{1}{n_2} \sum_{k=1}^{n_2-1} \mathbf{V}_k \mathbf{V}_k^T$, where $\mathbf{V}_k =: (V_{k1}, \dots, V_{kp})^T$, $1 \leq k \leq n_2 - 1$, are independent $N(0, \mathbf{I})$ random vectors. Set $\hat{\Sigma}_2^1 - \Sigma = \frac{1}{n_2} (\sum_{k=1}^{n_2-1} z_{kij})_{p \times p}$ and $\mathbf{v} = (v_1, \dots, v_p)^T$. We have

$$\begin{aligned} \langle (\hat{\Sigma}_2^1 - \Sigma) \mathbf{v}, \mathbf{v} \rangle &= \frac{1}{n_2} \sum_{k=1}^{n_2-1} \sum_{1 \leq i, j \leq p} v_i v_j z_{kij} \\ &= \frac{1}{n_2} \sum_{k=1}^{n_2-1} \left(\sum_{1 \leq i \leq p} v_i V_{ki} \right)^2 - 1 + n_2^{-1}. \end{aligned}$$

(26) is proved by the tail probability of χ^2 distribution. (27) follows from the exponential inequality in Lemma 1, Cai and Liu (2011). ■

Proof of Lemma 1 The objective is equivalent to (after neglecting constant terms with respect to β_p)

$$\beta_p \boldsymbol{\beta}_{-p}^T \Sigma_{12} + \frac{1}{2} \beta_p^2 \Sigma_{22} - \beta_p 1 \{p = i\} + \lambda |\beta_p|.$$

The minimizer of above should have a subgradient equal to zero,

$$\boldsymbol{\beta}_{-p}^T \Sigma_{12} + \beta_p \Sigma_{22} - 1 \{p = i\} + \lambda \text{sign}(\beta_p) = 0.$$

Thus the solution is given by the thresholding rule

$$\beta_p = \mathcal{T} (1 \{p = i\} - \boldsymbol{\beta}_{-p}^T \Sigma_{12}, \lambda) / \Sigma_{22}.$$

References

- [1] Banerjee, O., Ghaoui, L.E. and d'Aspremont, A. (2008). Model selection through sparse maximum likelihood estimation. *Journal of Machine Learning Research* 9: 485-516.
- [2] Bickel, P. and Levina, E. (2008). Covariance regularization by thresholding. *Annals of Statistics* 36: 2577-2604.
- [3] Borjabad, A., Morgello, S., Chao, W., Kim, S.-Y., Brooks, A.I., Murray, J., Potash, M.J., and Volsky, D.J. (2011). Significant effects of antiretroviral therapy on global gene expression in brain tissues of patients with HIV-1-associated neurocognitive disorders. *PLoS Pathog* 7(9): e1002213.
- [4] Breiman, Leo (2001). Random Forests. *Machine Learning* 45: 5-32.
- [5] Cai, T. and Liu, W. (2011), Adaptive thresholding for sparse covariance matrix estimation. *Journal of the American Statistical Association*, 106, 672-684.
- [6] Cai, T., Liu, W. and Luo, X. (2011), A constrained ℓ_1 minimization approach to sparse precision matrix estimation. *Journal of the American Statistical Association*, 106, 594-607.
- [7] Cai, T., Liu, W. and Zhou, H.H. (2011). Minimax rates of convergence for sparse inverse covariance matrix estimation. *Manuscript*.
- [8] Dickstein, D.P., Gorrostieta, C., Ombao, H., Goldberg, L.D., Brazel, A.C., Gable, C.J., Kelly, C., Gee, D.G., Zuo, X.N., Castellanos, F.X., and Michael, M.P. (2011).

Fronto-temporal spontaneous resting state functional connectivity in pediatric bipolar disorder. *Biological Psychiatry* 68: 839-846.

- [9] Fan, J., Feng, Y., and Wu, Y. (2009). Network exploration via the adaptive lasso and SCAD penalties. *Annals of Applied Statistics* 2: 521-541.
- [10] Fan, J. and Li, R. (2001). Variable selection via nonconcave penalized likelihood and its oracle properties. *Journal of American Statistical Association* 96: 1348-1360.
- [11] Friedman, J., Hastie, T. and Tibshirani, R. (2008). Sparse inverse covariance estimation with the graphical lasso. *Biostatistics* 9: 432-441.
- [12] Friedman, J., Hastie, T. and Tibshirani, R. (2008b). Regularization Paths for Generalized Linear Models via Coordinate Descent. *Journal of Statistical Software* 33: 1-22.
- [13] Guo, J., Levina, E., Michailidis, G. and Zhu, J. (2011). Joint estimation of multiple graphical models. *Biometrika* 98: 1-15.
- [14] Lam, C. and Fan, J. (2009). Sparsistency and rates of convergence in large covariance matrix estimation. *Annals of Statistics* 37: 4254-4278.
- [15] Lauritzen, S.L. (1996). Graphical models (*Oxford statistical science series*). Oxford University Press, USA.
- [16] Liu, H., Lafferty, J. and Wasserman, L. (2009). The nonparanormal: semiparametric estimation of high dimensional undirected graphs. *Journal of Machine Learning Research*. To appear.
- [17] Luo, X. (2011). High dimensional low rank and sparse covariance matrix estimation via convex minimization. Arxiv preprint arXiv:1111.1133.
- [18] Meinshausen, N. and Bühlmann, P. (2006). High-dimensional graphs and variable selection with the Lasso. *Annals of Statistics* 34: 1436-1462.
- [19] Ravikumar, P., Wainwright, M., Raskutti, G. and Yu, B. (2011). High-dimensional covariance estimation by minimizing l_1 -penalized log-determinant divergence. *Electronic Journal of Statistics* 5:935-980.
- [20] Rothman, A., Bickel, P., Levina, E. and Zhu, J. (2008). Sparse permutation invariant covariance estimation. *Electronic Journal of Statistics* 2: 494-515.

- [21] Tibshirani, R. (1996). Regression shrinkage and selection via the lasso. *Journal of the Royal Statistical Society. Series B* 58: 267-288.
- [22] Sun, T., and Zhang, C.H. (2012). Sparse matrix inversion with scaled lasso. Arxiv preprint arXiv:1202.2723.
- [23] Yuan, M. (2009). Sparse inverse covariance matrix estimation via linear programming. *Journal of Machine Learning Research* 11: 2261-2286.
- [24] Yuan, M. and Lin, Y. (2007). Model selection and estimation in the Gaussian graphical model. *Biometrika* 94: 19-35.
- [25] Zhou, S., van de Geer, S. and Bühlmann, P. (2009). Adaptive lasso for high dimensional regression and Gaussian graphical modeling. Arxiv preprint arXiv: 0903.2515.
- [26] Zou, H. (2006). The adaptive lasso and its oracle properties. *Journal of the American Statistical Association* 101: 1418-1429.